Shear flow behavior and dynamic viscosity of few-layer graphene nanofluids based on propylene glycol-water mixture

Samah Hamze, D. Cabaleiro, T. Mare, B. Vigolo, Patrice Estellé

Shear flow behavior and dynamic viscosity of few-layer graphene nanofluids based on propylene glycol-water mixture

Samah Hamze[1], David Cabaleiro[1,2], Thierry Maré[1], Brigitte Vigolo[3] and Patrice Estellé[1,*]

[1] Université de Rennes, LGCGM, F-35000 Rennes, France
[2] Dpto. Física Aplicada, Facultade de Ciencias, E-36310, Universidade de Vigo, Vigo, Spain
[3] Université de Lorraine, CNRS, Institut Jean Lamour UMR7198, F-54000 Nancy, France

* Correspondence: patrice.estelle@univ-rennes1.fr; Tel.: +33-0223234200 (P.E.)

Abstract: We report the shear flow behavior of few layer graphene (FLG) based nanofluids produced with a commercial mixture of water and propylene glycol and three nonionic surfactants, Triton X-100, Pluronic® P123, and Gum Arabic respectively. The flow properties of these nanofluids were experimentally investigated between 283.15-323.15 K and for FLG content from 0.05 to 0.5 wt.%. The nanofluids were subjected to different experiments, at rest at fixed temperature, under steady shear flow at fixed temperature and under temperature ramp at fixed shear rate in order to evaluate their stability and behavior under shear and temperature influence. These results were compared and correlated to visual aspect of the samples at the end of measurements. This experimental study evidences that the temperature, the shearing and the shearing duration have an important influence on the stability under shear of nanofluids in function of concentration and surfactant used. Finally, for all stable nanofluids under shear, the dynamic viscosity evolution of nanofluids with temperature is correlated to Vogel-Fulcher-Tammann model.

Keywords: Few-layer graphene nanofluids; propylene-glycol/water; shear flow stability; shear flow behavior; dynamic viscosity

1. Introduction

The progressive depletion of fossil fuels and world energy demand necessitate the development of new technologies based on alternative energy sources [1,2]. Nanofluids (nanoparticles dispersed in a conventional fluid) have become a research topic of immense interest worldwide. They have potential applications in many important fields such as in cooling technologies or advanced heat transfer, energy harvesting, medical, micro-electromechanical systems,

microfluidics, microelectronics, numerous thermal management systems and transportation [3–10]. Most studies have mainly focused on the determination of thermal properties of nanofluids, especially thermal conductivity, their modeling and their use in simulations, due to the potential benefits compared to suspensions of microparticles as well as conventional fluids [3,11–20]. Likewise, dynamic viscosity also becomes an important property when it comes to practical applications related to heat transfer and fluid flow. For instance, the pumping power, pressure drop and convective heat transfer in flow systems are directly dependent to the viscosity of the fluids. Consequently, the interest in investigation and analysis of nanofluid viscosity is recently growing than those regarding thermal conductivity which was the topic of extensive studies for a longer time [3]. Among the different types of nanoparticles used in literature, carbon-based nanomaterials, especially graphene, can be excellent thermal conductivity enhancers for nanofluid design, due to their excellent intrinsic thermal property compared to that of metal oxide or metallic nanoparticles [21–23].

Available literature shows that nanofluids can exhibit either a Newtonian or a non-Newtonian behavior, depending on nanoparticle shape, size or concentration [3,21,24]. Such an evaluation, as well as in what extend the viscosity of the base fluid is modified with the presence of graphene nanosheets, is of great interest for possible applications. With this aim, Moghaddam *et al.* [25] investigated graphene nanosheets with size of about 15-50 nm thick dispersed in glycerol. The prepared nanofluids were in the concentration range of 0.25-2.0 wt.%, and their viscosity was measured at temperatures between 293.15 and 323.15 K. A non-Newtonian behavior was reported by these authors and a strong enhancement in viscosity of glycerol by 401.49 % with the 2 wt.% loading of graphene nanosheets at shear rate 6.32 s^{-1} and at temperature equal to 293.15 K was also observed. On the other hand, Sarsam *et al.* [26] prepared 0.1 wt.% of graphene nanoplatelets (GNP)/water nanofluids without any surfactant assistance (samples labeled as “pristine” in that article) or stabilized using different surfactants like sodium dodecyl benzene sulfonate (SDBS), sodium dodecyl sulfate (SDS), cetyl trimethylammonium bromide (CTAB) and gum arabic (GA). Authors investigated the shear rate dependence of dynamic viscosity in the range from 20 to 200 s^{-1} and at temperatures from 298.15-328.15 K. Without any surfactant assistance, a slight shear thinning behavior was observed for nanofluid in the region of low shear rates for all studied temperatures expect for 308.15 K. A more remarkable pseudoplastic behavior was reported for the dispersions stabilized with GA (at a GA-

GNP ratio of 0.5:1) in the studied temperature range. Conversely, suspensions containing the ionic surfactants (SDBS, SDS and CTAB) at a surfactant-nanoparticle ratios of 1:1 behaved in a Newtonian manner. Additionally, the (1:1) SDBS-GNP sample showed the highest stability and nearly the lowest viscosity (7.4 % higher than distilled water). And based on the average values of viscosity, the water based nanofluids could be sequenced as (0.5:1) GA-GNPs >> pristine GNP > (1:1) SDBS-GNP > (1:1) SDS-GNP > (1:1) CTAB-GNP. The dispersion of GNPs, with thickness of about 5-10 nm and 15 μm of large dimension, in a mixture of deionized water:ethylene glycol (70:30 volume ratio) using 0.75 vol.% of sodium deoxycholate (SDC) as surfactant was studied by Selvam *et al.* [27]. The investigation was done for nanofluids in the GNP concentration range of 0.1-0.5 vol.%. The obtained results showed that the viscosity ratios (μ_{nf}/μ_{bf}) of nanofluids increased from 1.06 to 1.16 and 1.13 to 1.39 at 0.1 and 0.5 vol.%, respectively. In another work, Wang *et al.* [28] investigated single layer graphene (SLG)/water nanofluids that contain a special dispersant (not specified in the article). They found that the viscosity decreased with increasing temperature from 278.15 to 298.15 K increases with increasing concentration from 0.2 to 1 wt.% with a viscosity increment ratio between SLG nanofluids and water ranging from 1.24 to 2.35 and a non-Newtonian shear thinning behavior was reported. Vallejo *et al.* [29] studied functionalized GNP (fGNP) nanofluids based on water and propylene glycol:water mixture at 30:70 and 50:50 wt.%. Rheological investigation was performed at shear rates from 10 to 1000 s^{-1} with at different weight concentrations between 0.25 and 1 wt.% and in the temperature range 283.15-353.15 K. The authors obtained a non-Newtonian behavior at low shear rates (up to 100) and a Newtonian behavior at higher shear rates. Additionally, they found that in the case of base fluid with higher viscosity, the nanofluid viscosity decrease with temperature was higher and in the case of the base fluid with lower viscosity, the nanofluid viscosity increase with weight content of fGNP was higher.

On another hand, Vallejo *et al*. [30] investigated the rheological properties of sulfonic acid-fGNP nanofluids based on ethylene glycol:water mixture 50:50 vol%. Different weight concentrations of fGNPs in the range 0.25-2 % were prepared and studied in the shear rate range 1-1000 s^{-1} between 283.15 and 353.15 K. With increasing temperature within the tested range, the measurements showed a viscosity decrease by around 82 and 80 % for the base fluid and nanofluids, respectively. An increase in viscosity values was found with the increase of graphene loading. For example, a viscosity enhancement of 16 % was obtained for the nanofluid with 0.5

wt.% of fGNPs with respect to the base fluid, independently on the temperature. In addition, the studied nanofluids exhibited a shear thinning behavior at low shear rates with higher pseudoplasticity for higher graphene concentration; and a Newtonian behavior was found at higher shear rates.

In another study, functionalized fGNPs were dispersed in propylene glycol:water mixture at (30:70) wt% by Vallejo *et al.* [31]. The authors prepared nanofluids with weight content between 0.25 and 1 % and their viscosity was tested in the temperature range 293.15-323.15 K by imposing constant shear rates in the range of 1000-4000 s^{-1}. The viscosity was found independent on shear rate (Newtonian behavior) and on testing time (100 s). In addition, the temperature rise caused a decrease in viscosity between 31 and 57 %. On the other hand, with increasing the graphene loading, the viscosity increase attained 44 and 214 % for the lowest and highest fGNP concentration, respectively.

The rheological properties of graphene oxide (GO) and reduced graphene oxide (rGO)/water nanofluids were studied by Cabaleiro *et al.* [21] at 293.15 and 303.15 K. The prepared nanofluids were in the volume concentration range of 0.0005-0.1 %. The results showed a Newtonian behavior for the prepared nanofluids with graphene content lower than 0.01 vol.% and shear-thinning behavior was observed for higher graphene concentrations. Additionally, maximum increases of 100-130 % and 70-80 % was obtained respectively for the non-Newtonian GO and rGO based nanofluids. The largest increase was found for the highest concentration at 303.15 K. The results regarding the relative viscosity showed an enhancement by about 130 and 70% in the tested range of concentration for GO and rGO based nanofluids, respectively, without any significant influence of temperature. On the other hand, the authors showed that for the highest graphene content studied, rGO based nanofluids exhibited lower apparent viscosities than for GO-based nanofluids, and weaker shear-thinning behaviors.

In this study, high quality few layer graphene (FLG) was dispersed in a commercial mixture of propylene-glycol/water using three different nonionic surfactants, Pluronic® P-123, Triton X-100 and Gum Arabic. The studied nanoparticle weight concentrations are: 0.05, 0.1, 0.25, and 0.5 %. The rheological behavior of all corresponding base fluids and nanofluids were investigated at temperatures between 283.15 and 323.15 K and correlated to the visual aspect of the nanofluids after shearing. The results are discussed according to the influence of

concentration and type of surfactant, concentration of FLG, temperature and shearing time. For well-stable nanofluids under shear, the viscosity evolution with temperature and FLG concentration is finally predicted by a comprehensive viscosity model. This study is the last step of the thermophysical characterizations of these FLG-based nanofluids, as the stability at rest and thermal conductivity [32] and the volumetric and surface tension properties [33] were recently reported.

2. Materials and methods

As reported in our recent works [32,33], the nanofluids presently investigated are produced with high quality few-layer graphene (3-5 layers, mean lateral size 5µm, average thickness 1.5 nm) that was synthetized from ultrasound exfoliation of expanded graphene in water assisted by tannic acid. The full morphological and structural characterization of this FLG was previously performed in [32]. Graphene-based nanofluids were obtained from the dispersion of the FLG, previously washed, freezed and dried after the exfoliation process, in a commercial heat transfer fluid, namely Tyfocor® LS, that is a mixture of water and propylene glycol 60:40 wt.% using nonionic surfactants. Hence, Triton X-100 and Pluronic® P123 provided by Sigma Aldrich (Germany) and Gum Arabic by Acros Organics (France) were used as received. As also explained previously [32,33], a starting suspension with 0.5 wt.% of FLG was added to the base fluid, Tyfocor + surfactant (1 wt.%) and sonicated with a probe sonicator (Bioblock Scientific Vibra cell 75042, 125 W with a pulse mode 2 s ON / 1 s OFF) for several cycles of 15 min to avoid sample overheating. Samples with lower concentration were obtained from the dilution of the starting suspension with Tyfocor alone using the same sonication procedure. The surfactant:FLG ratio remain constant and equal to 2 for each FLG content that varies between 0.5 and 0.05 wt.%. The procedure was similarly followed for the three used surfactants. More details can be found in [32]. In the following, Pluronic® P-123, Triton X-100 and Gum Arabic will be referred to as P123, TrX and GA, respectively and Tyfocor is used in the text and the figures instead of Tyfocor® LS, for sake of clarity.

2.2 Rheological characterizations

Dynamic viscosity studies were performed on a Malvern Kinexus Pro rotational rheometer (Malvern Instruments Ltd., United Kingdom) equipped with a cone-plate geometry appropriate to investigate low-viscosity colloidal suspensions. The measuring geometry has a diameter of 60 mm and a cone angle of 1°, while the gap between the cone and the plate is 0.03 mm. Stress-controlled measurements were done at temperatures between 283.15 and 323.15 K with an interval of 10 K. Temperature was controlled with a precision of ±0.01 K by means of a Peltier temperature control device placed below the lower surface. Special thermal clovers were used to ensure constant temperature throughout the sample gap during experiments. A sample volume of 1 cm^3, considered optimal for the analysis with this geometry, was placed on the lower plate and a stabilization time of 5 min was allowed before experiments. Before starting the rheological measurements and in order to evaluate the temperature effect on nanofluid state at rest, every nanofluid was tested under controlled temperature at each single studied temperature for 10 minutes (+5 min stabilization time) and without shearing the sample.

Afterwards, two rheological analyses were performed. First, shear-viscosity flow curves were collected in state regimen at shear stresses in logarithmic scale corresponding to shear rates between 10 and 1000 s^{-1}. Finally, with the aim of analyzing the combined effect of both temperature and shearing time on nanofluid state, samples were also subject to a temperature ramp (in which temperature was continuously increased in the range from 283.15 to 323.15 K by steps of 10 K) while shear rate was hold to 500 s^{-1}. This shear rate was selected based on shear flow curves and corresponded to the region where Newtonian plateau was reached for all samples.

In an original way, pictures of the samples were taken at the end of the measurements to evaluate the stability of the nanofluids and to correlate the shear flow behavior with the visual aspect of the nanofluids.

Additional details about the experimental device can be found in Halelfadl *et al.* [34]. Experiments for each fluid and nanofluid and studied conditions were performed at least in duplicate and obtained flow curves did not show any significant difference. To validate the experimental shear flow protocol described above, dynamic viscosity measurements were done between 283.15 and 313.15 K for distilled water and between 273.15 and 373.15 K for Tyfocor thermal fluid. As expected, the results showed a Newtonian behavior for these two fluids. To

confirm the accuracy of the measure instrument, our experimental results were compared with those reported in the literature. The absolute average deviation obtained with water was about 3.5% [35] and that of Tyfocor was less than 5 % [36] in the tested temperature range.

3. Results and discussion

3.1. Effect of surfactant on viscosity of propylene-glycol/water mixture

To evaluate the effect of surfactant (type and concentration) on the dynamic viscosity of Tyfocor, this transport property was investigated in the temperature range 283.15-323.15 K for surfactant-Tyfocor mixtures prepared at surfactant concentrations of 0.1, 0.2, 0.5 and 1.0 wt.% with either Triton X-100, Pluronic® P-123 or Gum Arabic. At the investigated conditions, all studied surfactant-Tyfocor mixtures (which were also used as base fluids) exhibited a Newtonian behavior. As an example, Figure 1 shows the obtained flow curves for the mixture of Tyfocor and 0.2 wt.% of Triton X-100 at 283.15, 303.15 and 323.15 K.

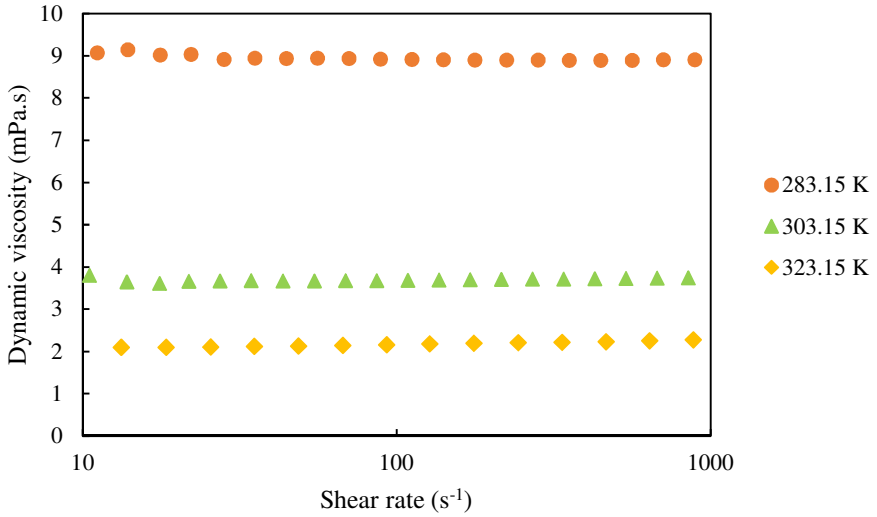

Figure 1. Flow curves for the base fluid Tyfocor and 0.2 wt.% of Triton X-100 at 283.15, 303.15 and 323.15 K.

Relative viscosity of the base fluids was determined in the tested temperature range as presented in Figure 2. The results show that the addition of Pluronic® P-123 (all concentrations), Triton X-100 (0.1, 0.2 and 0.5 wt.%) and Gum Arabic (0.1 and 0.2 wt.%) has no significant effect on the

viscosity of the starting fluid (Tyfocor) within the experimental uncertainty. The highest concentration of Triton X-100 (1 wt.%) increased the viscosity of Tyfocor by 7.9 % on average in the tested temperature range. With Gum Arabic, the dynamic viscosity was increased by 12.3 and 29.2 % after the addition of 0.5 and 1% of weight concentrations, respectively, without any dependence on the temperature.

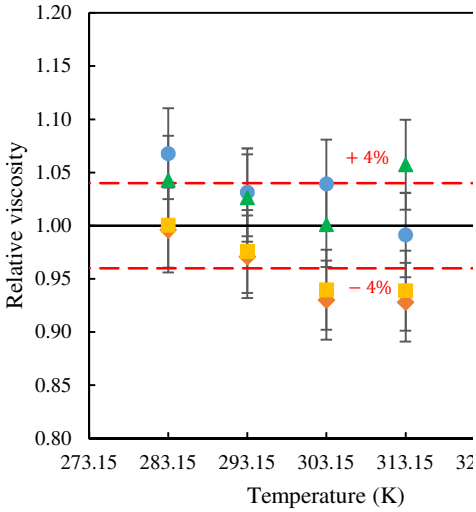

(a)

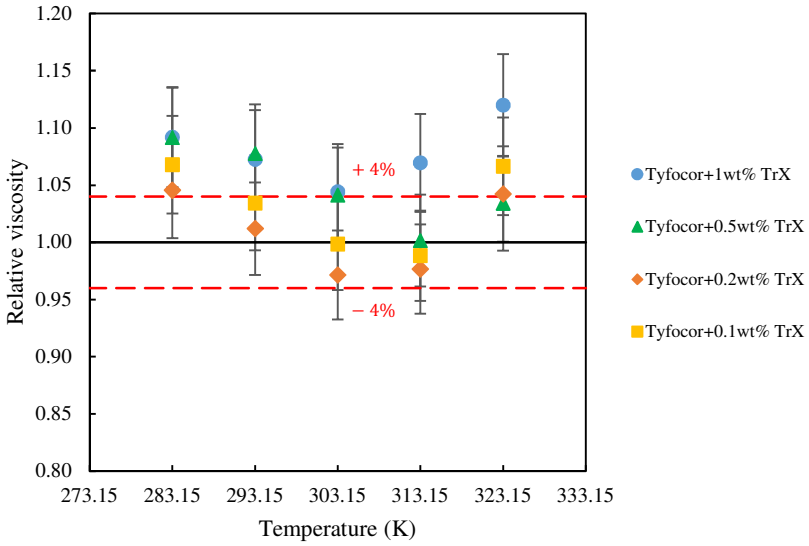

208

(b)

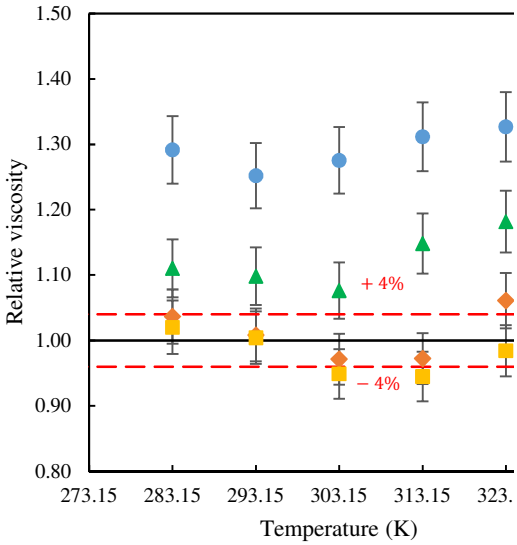

209

210

(c)

211

212 **Figure 2.** Relative viscosity of the studied base fluids prepared with Tyfocor with Pluronic® P-
213 123 (a), Triton X-100 (b), and Gum Arabic (c) as a function of temperature. Solid line represents
214 no viscosity enhancement for Tyfocor with surfactant compared to Tyfocor alone and dotted
215 lines at +/-4% represents the uncertainty in dynamic viscosity measurement.

216

217 **3.2 Effect of temperature and concentration on nanofluids behavior**

218 **3.2.1 Nanofluids at rest**

219 All the nanofluids produced with the three different surfactants were tested between 283.15 and
220 323.15 K, without and under shearing in order to discriminate between the temperature and the
221 shearing effects. The observed aspects of each nanofluids after each measurement are gathered in
222 Table 1. An example of each nanofluid state described in Table 1 is shown in Figure 3. Table 1
223 evidences that the dispersion state of the prepared FLG nanofluids can strongly vary after the
224 different experiments depending on the experimental protocol (no shear and shear), the type of

surfactant used, the temperature and the shearing time. Four states or aspects were mainly observed after the rheological measurements. The FLG-based nanofluids showing a dark homogeneous aspect without visible aggregates or with only few small aggregates, thus, appearing mainly as a well dispersed phase are named (⊕) for 'stable nanofluids' (Fig. 3a). When black FLG aggregates are visible, the aspect is noted aggregation (□) (Fig. 3b) and if these aggregates form a well-separated phase from the solvent, phase separation (▲) is recorded (Fig. 3d). In some cases, a homogeneous aspect is observed but in the form of a viscous gel (•) (Fig. 3c). Concisely, the FLG-based nanofluid samples produced with Pluronic® P-123 and Gum Arabic were rather stable at rest, while the dispersion state of the nanofluids prepared with Triton X-100 seemed much more sensitive to temperature. An aggregation phenomenon and a clear phase separation were indeed noticed when temperature increased especially for the highest FLG concentration.

Table 1. Observed states of the prepared nanofluid series at the end of the rheological measurements. Each visible aspect are noticed as (⊕) for the stable nanofluids without or with visually observed small aggregates, (□) for visible aggregates, (•) for a gel-like aspect, (▲) for a noticeable phase separation between FLG and the base fluid, (-) no measurement was done, (◊) no available photo. An example of each state mentioned in this table is shown in Fig. 3.

		T fixed, shear rate fixed at 0 s^{-1}					T fixed, shear rate ↑					T ↑, shear rate fixed at 500 s^{-1}				
	T(K) / φ_m	283.15	293.15	303.15	313.5	323.15	283.15	293.15	303.15	313.15	323.15	283.15	293.15	303.15	313.15	323.15
P123	0.05%	⊕	⊕	⊕	⊕	⊕	⊕	-	-	-	⊕	◊	◊	◊	◊	⊕
	0.1%	⊕	⊕	⊕	⊕	⊕	⊕	-	-	-	⊕	◊	◊	◊	◊	⊕
	0.25%	⊕	⊕	⊕	⊕	⊕	⊕	-	-	-	⊕	◊	◊	◊	◊	⊕
	0.5%	⊕	⊕	⊕	⊕	⊕	⊕	-	-	-	⊕	◊	◊	◊	⊕	•
TrX	0.05%	□	□	□	□	▲	□	□	▲	▲	▲	◊	◊	◊	◊	▲
	0.1%	⊕	⊕	⊕	□	□	⊕	⊕	⊕	▲	-	◊	◊	◊	▲	-
	0.25%	⊕	⊕	⊕	⊕	▲	⊕	⊕	⊕	•	▲	◊	◊	⊕	•	-
	0.5%	⊕	⊕	⊕	⊕	•	⊕	•	•	-	-	◊	◊	•	-	-
GA	0.05%	⊕	⊕	⊕	⊕	⊕	⊕	-	-	-	⊕	◊	◊	◊	◊	□

	0.1%	⊕	⊕	⊕	⊕	⊕	⊕	-	-	⊕	⊕	◊	◊	◊	◊	□
	0.25%	⊕	⊕	⊕	⊕	⊕	⊕	⊕	⊕	⊕	□	◊	◊	⊕	□	-
	0.5%	⊕	⊕	⊕	⊕	□	⊕	⊕	⊕	□	-	◊	◊	●	-	-

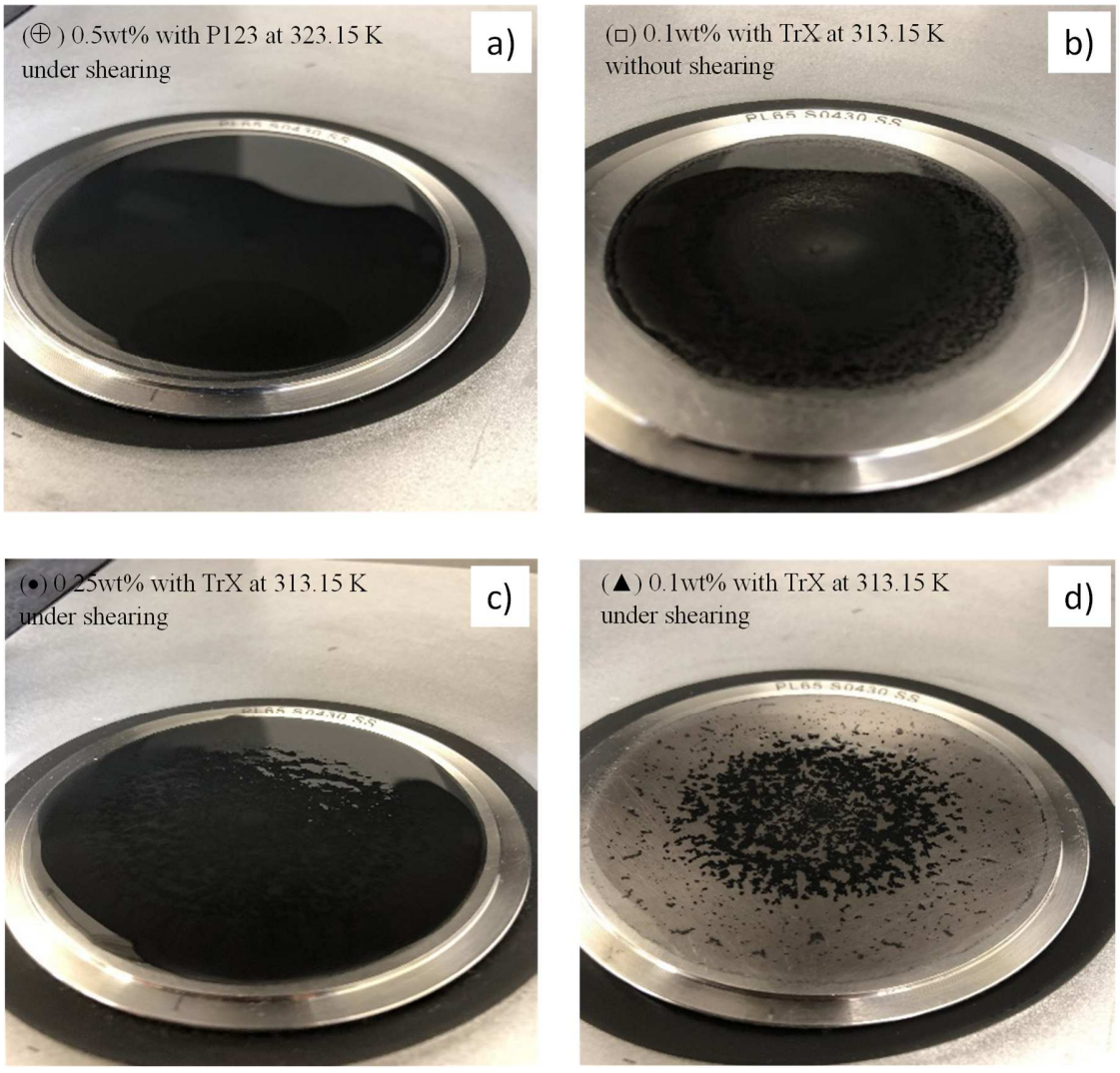

Figure 3. Representative examples of the different nanofluid states observed after performing the measurements: a) stable nanofluids without or with visually observed small aggregates (⊕), b) visible aggregates unseparated to the base fluid (□), c) gel-like aspect (●), and d) visible phase separation between the FLG aggregates and the solvent (▲).

3.2.2 Nanofluid under shear

The shear flow behavior of the prepared FLG-based nanofluids is discussed in the following considering the type of surfactant used and the FLG concentration. With Pluronic® P-123, the FLG-based nanofluids were mainly Newtonian in the investigated temperature range and they exhibited a slight shear-thinning behavior at low shear rates. Such a shear-thinning trend is more pronounced at 0.5 wt.% in FLG as the dynamic viscosity decreases up to 200 s^{-1} before to reach a Newtonian plateau. In addition, as noticed in Table 1, they stayed stable during all shear flow measurements. From this rheological study, the dynamic viscosity was found to increase with the FLG content in the nanofluids and to decrease with temperature.

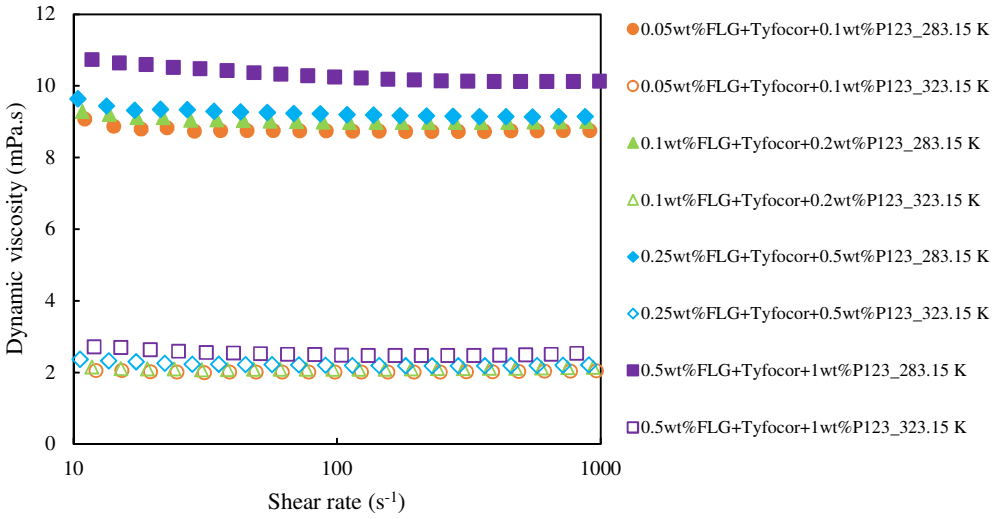

Figure 4. Dynamic viscosity of nanofluids with Pluronic® P-123 at 283.15 and 323.15 K as a function of shear rate.

FLG-based nanofluids prepared with Triton X-100 were observed to lose their stability at high temperature at rest (Table 1). Viscosity measurements with varying the shear rate between 10 and 1000 s^{-1} showed the shear flow behavior of the samples at the selected temperatures. The results of stable (dispersed state) nanofluids under shearing are presented in Figure 5(a), those showing a gel-like appearance at end of the measurement (Table 1) are shown in Figure 5(b). The stable FLG-based nanofluids behave as Newtonian fluids in the tested shear rate range with

a slight decrease in viscosity at very low shear rates indicating a weak shear-thinning. For the other FLG-based nanofluids after a slight reduction at very low shear rates, it is observed that the dynamic viscosity mainly increases with increasing shear rate indicating a shear-thickening behavior. This behavior under shearing can be related to the observed gelation phenomenon and the presence of a disordered structure of aggregates. This behavior seems to be sensitive to high temperature and concentration. Actually, it produces for the FLG nanofluids having a relatively high amount of surfactant and FLG (see also Table 1) *i.e.* 0.25 wt.% of FLG (and 0.5 wt.% of Triton X-100) at 323.15 K or for the suspensions containing 0.5 wt.% of FLG (and 1 wt.% of Triton X-100) at 293.15 and 303.15 K.

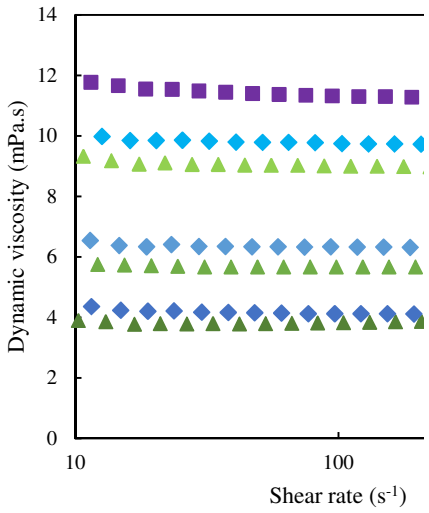

(a)

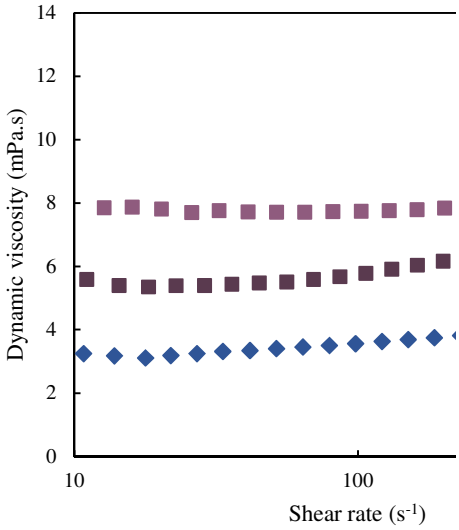

(b)

Figure 5. Dynamic viscosity of FLG-based nanofluids prepared with Triton X-100 between 283.15 and 313.15 K as a function of shear rate; FLG based nanofluids showing a (a) stable or dispersed state and a (b) gel-like aspect.

In the case of nanofluids prepared with Gum Arabic, they were stable with the presence of some aggregates for high FLG concentrations at high temperatures without shearing. After shearing measurements at selected temperatures, no significant change of their aspect was observed. These measurements showed different behaviors for these nanofluids, like quite Newtonian (Fig. 6a and 6b), or shear-thinning and shear-thickening at low shear rates up to 200 s^{-1} (Fig. 6b) before to reach a Newtonian plateau. For example, a slight shear-thinning behavior was obtained for 0.1 wt.% of Gum Arabic at 323.15 K, 0.25 wt.% of Gum Arabic at 303.15 K and 313.15 K and also for 0.5 wt.% of Gum Arabic at 283.15 K,respectively. A significant shear-thickening behavior was noticed for the highest concentration of FLG 0.5 w.t% (containing 1 wt.% of Gum Arabic) at 293.15 and 303.15 K at low shear rates (<200 s^{-1}). This trend could be attributed to the organization of the aggregates (see Table 1) under shear before to reach a stabilized state.

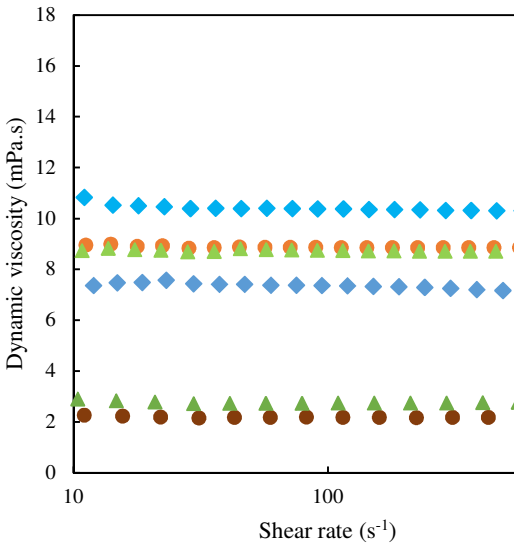

297

298 (a)

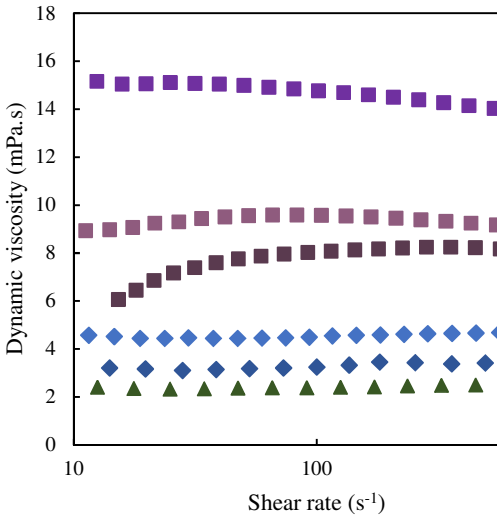

299

300 (b)

301

302 **Figure 6.** Dynamic viscosity of FLG based nanofluids prepared with Gum Arabic between
303 283.15 and 323.15 K as a function of shear rate; (a) Newtonian and (b) non- Newtonian samples.

The fact that certain Newtonian fluids become non-Newtonian after the dispersion of nanoparticles can be explained by the formation of possible nanoparticle-based fluid networks whose structure gets modified under shear stress [30,37–39]. Accordingly, a shear thinning behavior could indicate that nanoparticle networks could break once oriented in the flow direction of the shear. This would lessen the interaction forces, decreasing the flow resistance and, consequently, the apparent viscosity of the dispersion decreases [30,37–39]. Inversely, and as mentioned earlier, shear-thickening could be attributed the presence of the disordered structure of aggregates and their interaction.

3.2.3 Effect of shearing time and temperature

As explained before, a last measurement was performed with all stable nanofluids, selected from the previous experiments, by applying a fixing shear rate of 500 s^{-1} (this shear rate being in the Newtonian region) and increasing the temperature from 283.15 to 323.15 K with the same sample.

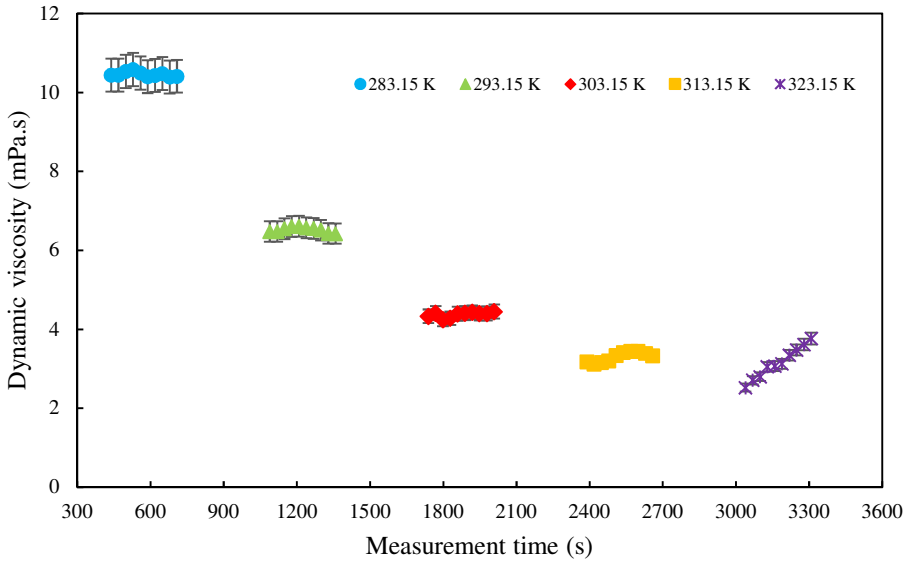

Figure 7. Dynamic viscosity of the nanofluid prepared with 0.5 wt.% of FLG and 1wt% Pluronic® P-123 between 283.15 and 323.15 K as a function of measurement time.

Concerning the nanofluids prepared with Pluronic® P-123, the dynamic viscosity was stable with time at all the temperatures between 283.15 and 323.15 K. However, with the highest

concentration of 0.5 wt.% of FLG, Figure 7 shows that the viscosity started to increase at 323.15 K after 3040 s from the beginning of the measurement e.g. after a total shearing time equal to 1200 s due to delay between each temperature change)and the sample looked like a gel at the end of measurement. Another measurement performed from 283.15 to 313.15 K did not show any significant change in the state of the nanofluid, which may indicate that such increase in viscosity at 323.15 K may be related to the instability of the sample and change in structure. Similar phenomenon was observed with the other two series, an increasing in the dynamic viscosity with time related to the loss of nanofluid stability after a certain shearing time and from certain temperature. Taking as an example the nanofluids prepared with Triton X-100, an increasing in viscosity is observed at measurement time equal to 2390 s, 1960 s, and 499.6 s (total shearing time equal to 900, 720 and 90 s) and that produces at the temperature 313.15, 303.15 and 283.15 K for the FLG concentrations of 0.1, 0.25 and 0.5 wt.%, respectively. With Gum Arabic nanofluids, the rise in viscosity was detected at measurement times equal to 3210, 3190, 1220, and 656 s (that corresponds to a total shearing times equal to 1440, 1380, 450 and 240s respectively) which corresponds to the temperatures of 323.15, 323.15, 293.15 and 283.15 K for the FLG concentrations of 0.05, 0.1, 0.25 and 0.5 wt.%, respectively. From Table 1, the difference between the nanofluid states observed with the three different kinds of measurements evidences that the temperature, the concentration, the shearing and the duration of shearing have an important role in the stability of nanofluids under shear. Based on the analysis compiled in Table 1, the nanofluid samples produced with Pluronic® P-123 seem to be the most resistant against shear and temperature. Nanofluids with Gum Arabic are relatively stable while nanofluids containing Triton X-100 have the lowest stability. It should be finally noted that the viscosities of the base fluids (mixtures of Tyfocor and surfactant) are not sensitive to this kind of test and all the values were stable with time and for all the temperatures from 283.15 to 323.15 K.

3.3 Nanofluid viscosity

Now to compare the results of the two different measurements for stable nanofluids, by fixing the temperature with increasing the shear rate from 10 to 1000 s^{-1} and by fixing the shear rate at 500 s^{-1} with increasing the temperature, the obtained viscosity values are represented in Fig. 8.

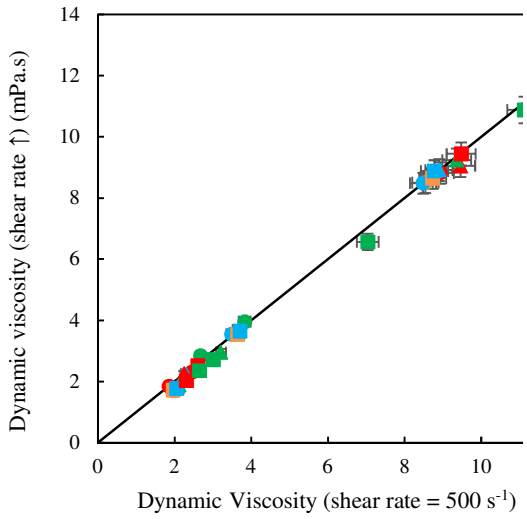

(a)

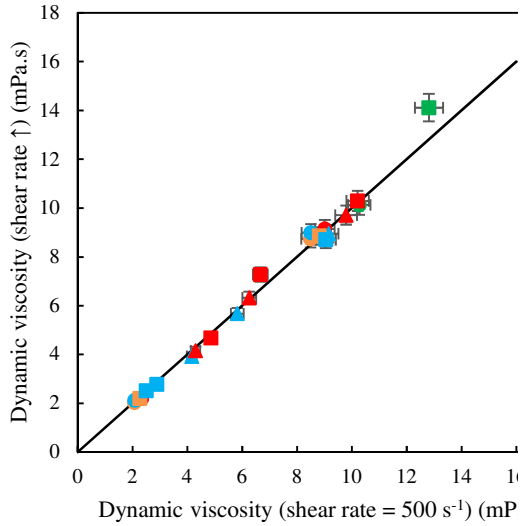

(b)

Figure 8. Comparison between the dynamic viscosity with varying shear rate and fixing it at 500 s^{-1} at different temperatures for the base fluids (a) and the corresponding FLG nanofluids (b). The solid line represents the bisector.

In figure 8, the viscosity results obtained from flow curve experiments (y-axis) correspond to the average value of data collected at shear rates higher than 200 s^{-1} (common Newtonian region for all stable nanofluids). Regarding the temperature ramps at a constant shear rate of 500 s^{-1} (x-axis), viscosity values are the average of all data that were constant during the measurement (before the rise in viscosity observed at certain temperatures as explained before). Fig. 8 shows clearly that these two different tests are compatible since they lead to values belonging quite well to same bisector (taking into account the experimental uncertainty). That is why in the following section, the considered viscosity values are the average of the results obtained with the two tests.

The effect of temperature on the viscosity of both base fluids and nanofluids is shown in Fig. 9. It is known that increasing temperature leads to decrease the viscosity of a fluid. This universal behavior in liquids is attributed to the lessening of molecular cohesive forces with increasing temperature, which reduces the shear stress and then the viscosity [40]. For all the studied base fluids and nanofluids, as expected, dynamic viscosity decreases with the increase of temperature in the range 283.15-323.15 K. The decreasing rate with Tyfocor alone and all base fluids is around 74 % from 283.15 to 323.15 K. For the nanofluids, the dynamic viscosity decreases with a similar trend as the corresponding base fluids, except for the highest concentration of FLG (0.5 wt%) with Gum Arabic where it decreases from 293.15 to 303.15 K by 9 %, while this rate is 30 % for the corresponding base fluid.

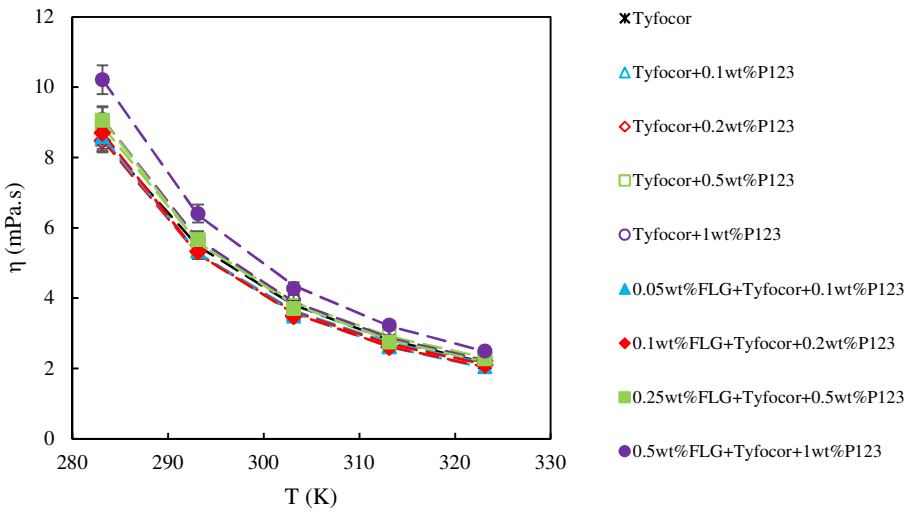

378

(a)

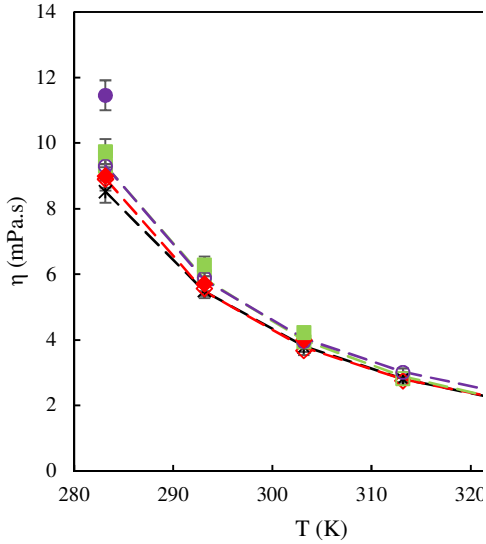

379

380

(b)

381

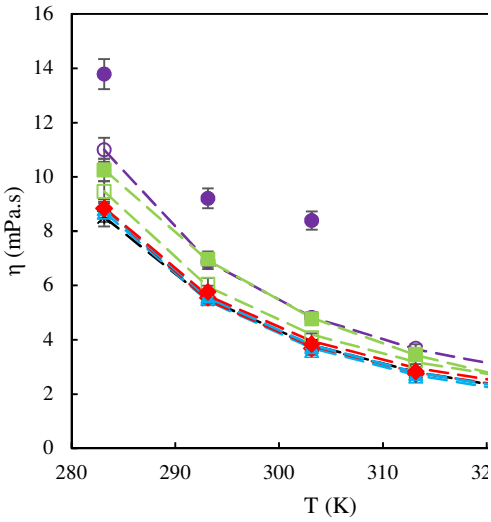

382

383

(c)

384

Figure 9. Dynamic viscosity of the FLG based nanofluids and the corresponding base fluids with Pluronic® P-123 (a), Triton X-100 (b) and Gum Arabic (c) as a function of temperature. The dashed lines represent the fitted values from Eq. 1.

One of the most used models describing the temperature dependence of viscosity is the Vogel-Fulcher-Tammann (VFT) equation [30,41–43]. This model has been previously used for graphene nanofluids [29,30,44].

$$\eta = \eta_0 \times e^{\frac{A \times T_0}{T - T_0}} \qquad (1)$$

where η_0, A, and T_0 are the fitting parameters. These parameters are gathered in Table 2 for both base fluids and nanofluids (that have results at more than three temperatures). Low absolute average deviations (AADs) and standard deviations between the experimental and fitted values around 1.53 % and 0.0961 mPa.s in average were obtained, respectively.

Table 2. Dynamic viscosity values (η) for base fluids and nanofluids and fitting parameters (η_0, A, and T_0), standard deviation (s) and AAD obtained from the VFT equation, Eq. (1).

Sft	$\varphi_{m,sft}$	$\varphi_{m,np}$	**Temperature (K)**					**Fitting parameters and deviations**				
	%	%	283.15	293.15	303.15	313.15	323.15	η_0 (mPa.s)	A	T_0 (K)	s (mPa.s)	AAD (%)
	0	0	8.52	5.48	3.81	2.81	2.17	0.0906	2.22	190.28	0.022	0.28
P123	0.1	0	8.538	5.272	3.646	2.725	2.153	0.2296	1.08	218.15	0.131	2.47
	0.2	0	8.500	5.242	3.614	2.690	2.116	0.2069	1.15	216.26	0.131	2.49
	0.5	0	8.889	5.582	3.891	2.917	2.306	0.2237	1.19	214.01	0.091	1.13
	1	0	9.094	5.669	3.895	2.870	2.228	0.1479	1.54	206.01	0.073	1.22
	0.1	0.05	8.603	5.269	3.576	2.612	2.015	0.1306	1.52	207.74	0.083	1.17
	0.2	0.1	8.710	5.257	3.567	2.624	2.044	0.1850	1.18	216.85	0.088	1.42
	0.5	0.25	9.082	5.581	3.815	2.811	2.188	0.1724	1.34	211.73	0.121	2.07
	1	0.5	10.222	6.357	4.359	3.206	2.485	0.1611	1.56	205.76	0.068	0.80
TrX	0.2	0	8.918	5.482	3.766	2.795	2.192	0.2053	1.18	215.65	0.106	1.84
	0.5	0	9.309	5.862	3.989	2.882	2.181	0.0597	2.72	183.97	0.087	1.57
	1	0	9.318	5.822	4.044	3.024	2.385	0.2271	1.20	214.10	0.092	1.29
GA	0.1	0	8.708	5.426	3.700	2.696	2.067	0.0971	1.93	198.09	0.118	1.99
	0.2	0	8.844	5.455	3.765	2.808	2.213	0.2265	1.11	217.32	0.123	2.22
	0.5	0	9.468	5.961	4.197	3.187	2.553	0.3259	0.96	220.33	0.107	1.28
	1	0	10.997	6.891	4.830	3.653	2.916	0.3552	0.99	219.72	0.032	0.42
	0.1	0.05	8.844	5.542	3.810	2.802	2.168	0.1254	1.71	202.06	0.085	1.49
	0.2	0.1	8.871	5.630	3.948	2.969	2.351	0.2210	1.24	211.95	0.195	3.40
	0.5	0.25	10.971	6.926	4.813	3.436	2.512	0.0005	58.11	41.30	0.0707	0.58

The decrease in viscosity with increasing temperature has also been found previously with graphene-based nanofluids with water [21,45–51] and glycoled water mixtures in different proportions [23,31,44,52,53], respectively.

Addition of nanoparticles to a liquid was reported to induce an increase in fluid resistance to flow because of the greater friction occurring within the mixture [44,54]. Thus, once a nanofluid flows, to overcome this augmentation in internal friction resistance a higher energy consumption is required (in comparison to the base fluid without nanoparticles) [35,54]. Hence, the addition of nanoparticles in a liquid increases its viscosity. The viscosity enhancement of the studied stable FLG based nanofluids under shear as function of FLG concentration and temperature is shown in Fig. 10.

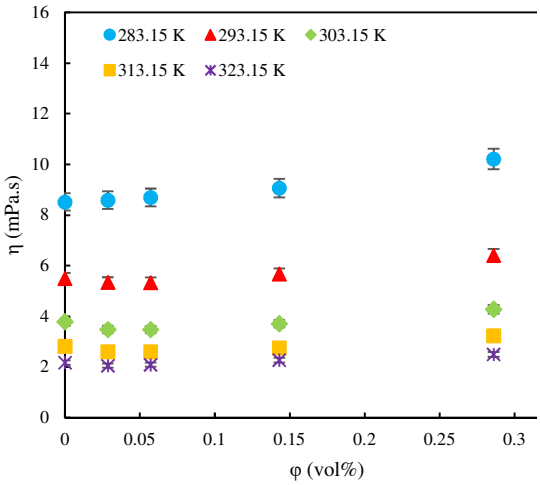

(a)

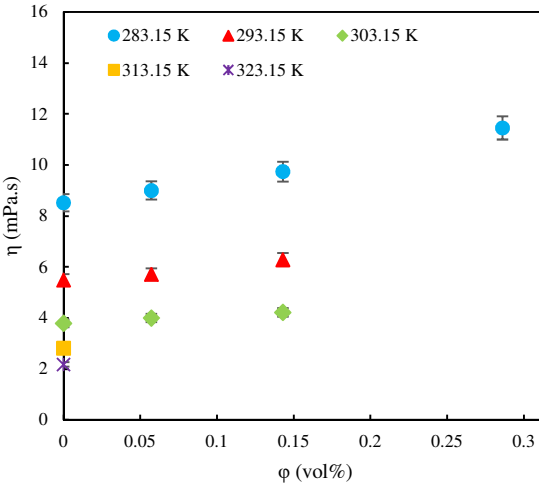

(b)

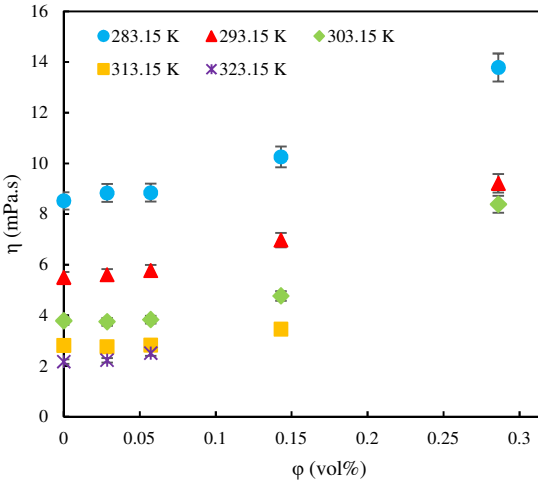

(c)

Figure 10. Dynamic viscosity of the FLG-based nanofluids with Pluronic® P-123 (a), Triton X-100 (b) and Gum Arabic (c) as a function of FLG volume concentration.

It worth noting that the volume concentration φ, used in Fig.10 is calculated from the $\varphi_m$using the following equation [32]:

$$\varphi = \frac{\varphi_m \times \frac{\rho_{bf}}{\rho_{np}}}{\left(1-\varphi_m \times \left(1-\frac{\rho_{bf}}{\rho_{np}}\right)\right)} \qquad (2)$$

where ρ_{bf} and ρ_{np} are the experimental densities of base fluids at all temperatures and the one of the nanoparticles at ambient temperature, respectively, as reported in [33]. The increase rate in dynamic viscosity (with respect to Tyfocor fluid) is maximal for the highest FLG tested concentrations. Thus, it reaches 19.9, 34.5 and 121.6 % in the case of Pluronic® P-123, Triton X-100 and Gum Arabic at 283.15, 283.15 and 303.15 K, respectively for the nanofluids containing 0.5 wt.% of FLG. From an insight of Fig.10, it can be observed that the nanofluids with Pluronic® P-123 have lower viscosities than samples containing Triton X-100 and the highest viscosities were obtained for Gum Arabic series.

4. Concluding remarks

This study concerned the rheological characterization of FLG-based nanofluids produced with a commercial heat transfer fluid based on a mixture of water and propylene glycol and different non-ionic surfactants. In an original way, nanofluid samples were subjected to different experiments, at rest at fixed temperature, under steady shear flow at fixed temperature and under temperature ramp at fixed shear rate, which allowed to evaluate their stability and behavior under shear and temperature influence. These results were compared and correlated to visual aspect of the sample at the end of measurements. These experiments were performed in the temperature range 283.15-323.15 K and varying the mass content in FLG from 0.05 to 0.5 %. The difference between the nanofluids states observed with the different measurement methods showed that the temperature, the shearing and the duration of shearing have an important role on the nanofluids stability in function of their concentration and surfactant. This also allows the best nanofluid and surfactant to be evaluated in terms of stability under flow. Finally, for the stable nanofluids under shear, the dynamic viscosity evolution with temperature was correlated to Vogel-Fulcher-Tammann (VFT) equation.

Acknowledgements:

The authors would like to thank Dr. D. Bégin for providing FLG samples, Dr. N. Berrada for her help in the preparation of the FLG based nanofluids and Dr. A. Desforges for fruitful discussions. D.C. is recipient of a postdoctoral fellowship from Xunta de Galicia (Spain). This investigation is a contribution to the COST (European Cooperation in Science and Technology) Action CA15119: Overcoming Barriers to Nanofluids Market Uptake (NanoUptake).

References

[1] M. Mehrali, S. Tahan Latibari, M.A. Rosen, A.R. Akhiani, M.S. Naghavi, E. Sadeghinezhad, H.S.C. Metselaar, M. Mohammadi Nejad, M. Mehrali, From rice husk to high performance shape stabilized phase change materials for thermal energy storage, RSC Adv. 6 (2016) 45595–45604. https://doi.org/10.1039/C6RA03721F.

[2] S. Iranmanesh, H.C. Ong, B.C. Ang, E. Sadeghinezhad, A. Esmaeilzadeh, M. Mehrali, Thermal performance enhancement of an evacuated tube solar collector using graphene nanoplatelets nanofluid, J. Clean. Prod. 162 (2017) 121–129. https://doi.org/10.1016/j.jclepro.2017.05.175.

[3] S.M.S. Murshed, P. Estellé, A state of the art review on viscosity of nanofluids, Renew. Sustain. Energy Rev. 76 (2017) 1134–1152. https://doi.org/10.1016/j.rser.2017.03.113.

[4] S.U.S. Choi, Z.G. Zhang, P. Keblinski, Nanofluids. In: Nalwa HS, editor. Encyclopedia of nanoscience and nanotechnology. Los Angeles: American Scientific Publishers; 2004. p. 757–73.

[5] S.K. Das, ed., Nanofluids: science and technology, Wiley-Interscience, Hoboken, N.J, 2008.

[6] S.M.S. Murshed, K.C. Leong, C. Yang, Thermophysical and electrokinetic properties of nanofluids – A critical review, Appl. Therm. Eng. 28 (2008) 2109–2125. https://doi.org/10.1016/j.applthermaleng.2008.01.005.
[7] K.V. Wong, O. De Leon, Applications of nanofluids: Current and future, Adv. Mech. Eng. 2 (2010) 519659. https://doi.org/10.1155/2010/519659.
[8] R. Saidur, K.Y. Leong, H.A. Mohammed, A review on applications and challenges of nanofluids, Renew. Sustain. Energy Rev. 15 (2011) 1646–1668. https://doi.org/10.1016/j.rser.2010.11.035.
[9] S.M.S. Murshed, C.A.N. de Castro, Nanofluids as Advanced Coolants, in: Inamuddin, A. Mohammad (Eds.), Green Solvents I, Springer Netherlands, Dordrecht, 2012: pp. 397–415. https://doi.org/10.1007/978-94-007-1712-1_14.
[10] S.M.S. Murshed, C.A.N. de Castro, eds., Nanofluids: synthesis, properties, and applications, Nova Science Publishers, Inc, New York, 2014.
[11] W. Yu, D.M. France, J.L. Routbort, S.U.S. Choi, Review and comparison of nanofluid thermal conductivity and heat transfer enhancements, Heat Transf. Eng. 29 (2008) 432–460. https://doi.org/10.1080/01457630701850851.
[12] S. Thomas, C. Balakrishna Panicker Sobhan, A review of experimental investigations on thermal phenomena in nanofluids, Nanoscale Res. Lett. 6 (2011) 377. https://doi.org/10.1186/1556-276X-6-377.
[13] S. Özerinç, S. Kakaç, A.G. Yazıcıoğlu, Enhanced thermal conductivity of nanofluids: a state-of-the-art review, Microfluid. Nanofluidics. 8 (2010) 145–170. https://doi.org/10.1007/s10404-009-0524-4.
[14] O. Mahian, L. Kolsi, M. Amani, P. Estellé, G. Ahmadi, C. Kleinstreuer, J.S. Marshall, M. Siavashi, R.A. Taylor, H. Niazmand, S. Wongwises, T. Hayat, A. Kolanjiyil, A. Kasaeian, I. Pop, Recent advances in modeling and simulation of nanofluid flows-Part I: Fundamentals and theory, Phys. Rep. 790 (2019) 1–48. https://doi.org/10.1016/j.physrep.2018.11.004.
[15] O. Mahian, L. Kolsi, M. Amani, P. Estellé, G. Ahmadi, C. Kleinstreuer, J.S. Marshall, R.A. Taylor, E. Abu-Nada, S. Rashidi, H. Niazmand, S. Wongwises, T. Hayat, A. Kasaeian, I. Pop, Recent advances in modeling and simulation of nanofluid flows—Part II: Applications, Phys. Rep. 791 (2019) 1–59. https://doi.org/10.1016/j.physrep.2018.11.003.
[16] S.M.S. Murshed, K.C. Leong, C. Yang, Thermophysical properties of nanofluids. In: Sattler KD, editor. Handbook of nanophysics: nanoparticles and quantum dots. Boca Raton: Taylor & Francis; 2010.
[17] C. Kleinstreuer, Y. Feng, Experimental and theoretical studies of nanofluid thermal conductivity enhancement: a review, Nanoscale Res. Lett. 6 (2011) 229. https://doi.org/10.1186/1556-276X-6-229.
[18] S.M.S. Murshed, C.A. Nieto de Castro, Superior thermal features of carbon nanotubes-based nanofluids – A review, Renew. Sustain. Energy Rev. 37 (2014) 155–167. https://doi.org/10.1016/j.rser.2014.05.017.
[19] H.Ş. Aybar, M. Sharifpur, M.R. Azizian, M. Mehrabi, J.P. Meyer, A review of thermal conductivity models for nanofluids, Heat Transf. Eng. 36 (2015) 1085–1110. https://doi.org/10.1080/01457632.2015.987586.
[20] P. Estellé, S. Halelfadl, T. Maré, Thermal conductivity of CNT water based nanofluids: Experimental trends and models overview, J. Therm. Eng. 1 (2015) 381. https://doi.org/10.18186/jte.92293.
[21] D. Cabaleiro, P. Estellé, H. Navas, A. Desforges, B. Vigolo, Dynamic viscosity and surface tension of stable graphene oxide and reduced graphene oxide aqueous nanofluids, J. Nanofluids. 7 (2018) 1081–1088. https://doi.org/10.1166/jon.2018.1539.
[22] A.A. Balandin, Thermal properties of graphene and nanostructured carbon materials, Nat. Mater. 10 (2011) 569–581. https://doi.org/10.1038/nmat3064.
[23] D. Cabaleiro, L. Colla, S. Barison, L. Lugo, L. Fedele, S. Bobbo, Heat transfer capability of (Ethylene Glycol + Water)-based nanofluids containing graphene nanoplatelets: Design and

515 thermophysical profile, Nanoscale Res. Lett. 12 (2017) 53. https://doi.org/10.1186/s11671-016-
516 1806-x.
517 [24] G. Żyła, Nanofluids containing low fraction of carbon black nanoparticles in ethylene glycol: An
518 experimental study on their rheological properties, J. Mol. Liq. 297 (2020) 111732.
519 https://doi.org/10.1016/j.molliq.2019.111732.
520 [25] M.B. Moghaddam, E.K. Goharshadi, M.H. Entezari, P. Nancarrow, Preparation, characterization,
521 and rheological properties of graphene–glycerol nanofluids, Chem. Eng. J. 231 (2013) 365–372.
522 https://doi.org/10.1016/j.cej.2013.07.006.
523 [26] W.S. Sarsam, A. Amiri, S.N. Kazi, A. Badarudin, Stability and thermophysical properties of non-
524 covalently functionalized graphene nanoplatelets nanofluids, Energy Convers. Manag. 116 (2016)
525 101–111. https://doi.org/10.1016/j.enconman.2016.02.082.
526 [27] C. Selvam, D. Mohan Lal, S. Harish, Enhanced heat transfer performance of an automobile radiator
527 with graphene based suspensions, Appl. Therm. Eng. 123 (2017) 50–60.
528 https://doi.org/10.1016/j.applthermaleng.2017.05.076.
529 [28] Y. Wang, H.A.I. Al-Saaidi, M. Kong, J.L. Alvarado, Thermophysical performance of graphene
530 based aqueous nanofluids, Int. J. Heat Mass Transf. 119 (2018) 408–417.
531 https://doi.org/10.1016/j.ijheatmasstransfer.2017.11.019.
532 [29] J.P. Vallejo, G. Żyła, J. Fernández-Seara, L. Lugo, Rheological behaviour of functionalized
533 graphene nanoplatelet nanofluids based on water and propylene glycol:water mixtures, Int.
534 Commun. Heat Mass Transf. 99 (2018) 43–53.
535 https://doi.org/10.1016/j.icheatmasstransfer.2018.10.001.
536 [30] J. Vallejo, G. Żyła, J. Fernández-Seara, L. Lugo, Influence of Six Carbon-Based Nanomaterials on
537 the Rheological Properties of Nanofluids, Nanomaterials. 9 (2019) 146.
538 https://doi.org/10.3390/nano9020146.
539 [31] J.P. Vallejo, J. Pérez-Tavernier, D. Cabaleiro, J. Fernández-Seara, L. Lugo, Potential heat transfer
540 enhancement of functionalized graphene nanoplatelet dispersions in a propylene glycol-water
541 mixture. Thermophysical profile, J. Chem. Thermodyn. 123 (2018) 174–184.
542 https://doi.org/10.1016/j.jct.2018.04.007.
543 [32] S. Hamze, N. Berrada, D. Cabaleiro, A. Desforges, J. Ghanbaja, J. Gleize, D. Bégin, F. Michaux, T.
544 Maré, B. Vigolo, P. Estellé, Few-layer graphene-based nanofluids with enhanced thermal
545 conductivity, Nanomaterials. 10 (2020) 1258. https://doi.org/10.3390/nano10071258.
546 [33] S. Hamze, D. Cabaleiro, D. Bégin, A. Desforges, T. Maré, B. Vigolo, L. Lugo, P. Estellé,
547 Volumetric properties and surface tension of few-layer graphene nanofluids based on a commercial
548 heat transfer fluid, Energies. 13 (2020) 3462. https://doi.org/10.3390/en13133462.
549 [34] S. Halelfadl, P. Estellé, B. Aladag, N. Doner, T. Maré, Viscosity of carbon nanotubes water-based
550 nanofluids: Influence of concentration and temperature, Int. J. Therm. Sci. 71 (2013) 111–117.
551 https://doi.org/10.1016/j.ijthermalsci.2013.04.013.
552 [35] J.V. Sengers, J.T.R. Watson, Improved international formulations for the viscosity and thermal
553 conductivity of water substance, J. Phys. Chem. Ref. Data. 15 (1986) 1291–1314.
554 https://doi.org/10.1063/1.555763.
555 [36] Tyfocor LS Technical Information available at https://tyfo.de/en/produkt/tyfocor-ls/, (n.d.).
556 [37] M. Pastoriza-Gallego, L. Lugo, J. Legido, M.M. Piñeiro, Rheological non-Newtonian behaviour of
557 ethylene glycol-based Fe2O3 nanofluids, Nanoscale Res. Lett. 6 (2011) 560.
558 https://doi.org/10.1186/1556-276X-6-560.
559 [38] S. Genc, B. Derin, Synthesis and rheology of ferrofluids: a review, Curr. Opin. Chem. Eng. 3 (2014)
560 118–124. https://doi.org/10.1016/j.coche.2013.12.006.
561 [39] C. Hermida-Merino, M. Pérez-Rodríguez, M.M. Piñeiro, M.J. Pastoriza-Gallego, Evidence of
562 viscoplastic behavior of exfoliated graphite nanofluids, Soft Matter. 12 (2016) 2264–2275.
563 https://doi.org/10.1039/C5SM02932E.
564 [40] J. F. Douglas, Fluid mechanics, 5th ed. Harlow, England ; New York : Pearson/Prentice Hall, 2006.

565 [41] G.S. Fulcher, Analysis of recent measurements of the viscosity of glasses, J. Am. Ceram. Soc. 8
566 (1925) 339–355. https://doi.org/10.1111/j.1151-2916.1925.tb16731.x.
567 [42] G. Tammann, W. Hesse, The dependence of viscosity upon the temperature of supercooled liquids.
568 Z. Anorg. Allg. Chem. 1926, 156, 245–257.
569 [43] H. Vogel, The law of the relation between the viscosity of liquids and the temperature. Phys. Z
570 1921, 22, 645–646.
571 [44] J.P. Vallejo, S. Gómez-Barreiro, D. Cabaleiro, C. Gracia-Fernández, J. Fernández-Seara, L. Lugo,
572 Flow behaviour of suspensions of functionalized graphene nanoplatelets in propylene glycol–water
573 mixtures, Int. Commun. Heat Mass Transf. 91 (2018) 150–157.
574 https://doi.org/10.1016/j.icheatmasstransfer.2017.12.001.
575 [45] P. Dhar, M.H.D. Ansari, S.S. Gupta, V.M. Siva, T. Pradeep, A. Pattamatta, S.K. Das, Percolation
576 network dynamicity and sheet dynamics governed viscous behavior of polydispersed graphene
577 nanosheet suspensions, J. Nanoparticle Res. 15 (2013) 2095. https://doi.org/10.1007/s11051-013-
578 2095-2.
579 [46] M. Mehrali, E. Sadeghinezhad, S. Latibari, S. Kazi, M. Mehrali, M.N.B.M. Zubir, H.S. Metselaar,
580 Investigation of thermal conductivity and rheological properties of nanofluids containing graphene
581 nanoplatelets, Nanoscale Res. Lett. 9 (2014) 15. https://doi.org/10.1186/1556-276X-9-15.
582 [47] E. Sadeghinezhad, M. Mehrali, S. Tahan Latibari, M. Mehrali, S.N. Kazi, C.S. Oon, H.S.C.
583 Metselaar, Experimental investigation of convective heat transfer using graphene nanoplatelet based
584 nanofluids under turbulent flow conditions, Ind. Eng. Chem. Res. 53 (2014) 12455–12465.
585 https://doi.org/10.1021/ie501947u.
586 [48] M. Mehrali, E. Sadeghinezhad, M.A. Rosen, S. Tahan Latibari, M. Mehrali, H.S.C. Metselaar, S.N.
587 Kazi, Effect of specific surface area on convective heat transfer of graphene nanoplatelet aqueous
588 nanofluids, Exp. Therm. Fluid Sci. 68 (2015) 100–108.
589 https://doi.org/10.1016/j.expthermflusci.2015.03.012.
590 [49] M. Mehrali, E. Sadeghinezhad, M.A. Rosen, A.R. Akhiani, S. Tahan Latibari, M. Mehrali, H.S.C.
591 Metselaar, Heat transfer and entropy generation for laminar forced convection flow of graphene
592 nanoplatelets nanofluids in a horizontal tube, Int. Commun. Heat Mass Transf. 66 (2015) 23–31.
593 https://doi.org/10.1016/j.icheatmasstransfer.2015.05.007.
594 [50] M.R. Esfahani, E.M. Languri, M.R. Nunna, Effect of particle size and viscosity on thermal
595 conductivity enhancement of graphene oxide nanofluid, Int. Commun. Heat Mass Transf. 76 (2016)
596 308–315. https://doi.org/10.1016/j.icheatmasstransfer.2016.06.006.
597 [51] M. Hadadian, E.K. Goharshadi, A. Youssefi, Electrical conductivity, thermal conductivity, and
598 rheological properties of graphene oxide-based nanofluids, J. Nanoparticle Res. 16 (2014) 2788.
599 https://doi.org/10.1007/s11051-014-2788-1.
600 [52] A. Ijam, R. Saidur, P. Ganesan, A. Moradi Golsheikh, Stability, thermo-physical properties, and
601 electrical conductivity of graphene oxide-deionized water/ethylene glycol based nanofluid, Int. J.
602 Heat Mass Transf. 87 (2015) 92–103. https://doi.org/10.1016/j.ijheatmasstransfer.2015.02.060.
603 [53] M. Kole, T.K. Dey, Investigation of thermal conductivity, viscosity, and electrical conductivity of
604 graphene based nanofluids, J. Appl. Phys. 113 (2013) 084307. https://doi.org/10.1063/1.4793581.
605 [54] Materials Science & Technology Conference et al., Éd., Processing and properties of advanced
606 ceramics and composites V. 2013.
607